Anion Dependence in the Partitioning between Proton and Electron Transfer in Ion/Ion Reactions

Joshua J. Coon,*[1,5] John E. P. Syka,*[2,3] Jae C. Schwartz,[3] Jeffrey Shabanowitz,[1] Donald F. Hunt,[1,4]

Departments of Chemistry[1] and Pathology[4], University of Virginia, Charlottesville, VA
Engineering Physics Program,[2] University of Virginia, Charlottesville, VA
Thermo Electron Corporation,[3] San Jose, CA

*J.J.C. and J.E.P.S. contributed equally to this work. [5]To whom correspondence should be addressed. Email: jcoon@virginia.edu. Phone: (434) 924-7994. Fax: (434) 982-2781. Dept. of Chemistry, Univ. of Virginia, McCormick Rd., Charlottesville, VA 22901

Keywords: electron transfer dissociation, electron capture dissociation, fragmentation, ion/ion reactions, charge transfer, ion trap

Abstract

Gas-phase reactions of singly-charged anions with multiply-protonated peptides, in a RF quadrupole linear ion trap, leads to either peptide deprotonation (proton transfer) or electron deposition (electron transfer). The former process induces peptide backbone cleavage through a reaction scheme analogous to electron capture dissociation (ECD). Here we characterize the preferred reaction pathways of several anions with multiply-protonated peptides. These anions include sulfur dioxide, perfluoro-1,3-dimethyl-cyclohexane, sulfur hexafluoride, anthracene, and 9,10 diphenylanthracene. In our ion/ion apparatus, we find some anions react exclusively via proton transfer, others react by proton and electron transfer, while another behaved predominantly as an electron transfer agent.

1. Introduction

Owing to its non-ergodic nature, electron capture dissociation (ECD), introduced by McLafferty and co-workers [1], has been unique among ion fragmentation methods. In ECD near-thermal electrons, contained by the magnetic field of a Fourier transform ion cyclotron resonance (FTICR) mass spectrometer, are captured by multiply-charged peptide/protein cations. The process induces cleavage of the amide nitrogen-alpha carbon bond to create c/z-type product ions, [2,3] while preserving labile post-translational modifications. [4-11] Unfortunately, simultaneous confinement of electrons and positive ions is not straightforward in other trapping mass analyzers, e.g., quadrupole ion traps; hence, ECD remains restricted to FTICR systems – unavailable to the vast majority of the biological mass spectrometry community.

Cations and anions can, however, be contained concurrently in radio frequency (RF) electrostatic trapping fields. By exploitation of this attribute, we recently reported the use of anions as vehicles for electron delivery to multiply-protonated peptides in a RF quadrupole linear (QLT) ion trap mass spectrometer [12]. In ECD, charge neutralization and hydrogen atom release results from the capture of near-thermal electrons by peptide cations (excitation energy ~ 6 eV) [13]. Likewise, the electron transfer reaction deposits sufficient excitation energy, only lowered by the electron affinity (EA) of the radical anion (0.5 – 1.5 eV, depending on the radical anion), for hydrogen atom liberation. [12] In either case, the net effect is production of mobile hydrogen atoms for subsequent recombination, producing c/z-type fragmentation.

Over the past decade McLuckey, Stephenson, and co-workers have pioneered ion/ion chemistry using three-dimensional (3D) quadrupole ion traps (QIT) [14-20]. Those experiments employ proton transfer reactions for peptide/protein charge neutralization [21-26]. This work was the primary, but not exclusive [27,28], basis for the prevailing view that multiply-charged peptides interact with anions exclusively via anion attachment or proton transfer. Our recent report extends ion/ion chemistry to contain a new reaction pathway: electron transfer [12]. Here we characterize the ion/ion chemistry of several anions with multiply-protonated peptides, as observed with our QLT ion/ion apparatus. Some of the anions were used by others (e.g., sulfur dioxide and perfluoro-1,3-dimethyl-cyclohexane); some of the anions were not (e.g., 9,10 diphenyl anthracene). In addition to anion characterization, we briefly comment on the differences between 3D RF quadrupole ion traps (QIT) and RF quadrupole linear ion traps (QLT) for ion/ion reactions.

2. Experimental

Multiply-protonated peptides were generated by electrospray ionization (ESI). A 40% aqueous acetonitrile solution (with 0.1% acetic acid), containing peptides at 1 pmol/μL, was infused into a SilicaTip™ fused silica emitter (30 μm tip, New Objective, Woburn, MA, USA). Peptides studied include angiotensin, neurotensin (Sigma-Aldrich, St. Louis, MO, USA), and the in-house synthesized phosphopeptide, LPISASHpSpSKTR.

A Finnigan LTQ linear ion trap mass spectrometer (Thermo Electron, San Jose, CA, USA) was adapted to accept a Finnigan 4500 chemical ionization source (FinniganMAT, Sunnyvale, CA, USA), which was mounted on the rear side of the device, opposing the factory nanospray source. Negative chemical ionization (NICI), with methane buffer gas (MG Industries, Malvern, PA, USA), was used to produce anions of sulfur dioxide, sulfur hexafluoride (MG Industries, Malvern, PA, USA), anthracene, perfluoro-1,3,-diphenyl-cyclohexane (PDCH), and 9,10 diphenyl anthracene (Sigma-Aldrich, St. Louis, MO, USA). Introduction of PDCH, anthracene, and 9,10 diphenylanthracene was accomplished via a batch inlet consisting of a gas chromatograph oven and a heated transfer line (Thermo Electron, Austin, TX).

For charge-sign-independent trapping the Finnigan LTQ electronics were modified to allow superposition of a secondary RF trapping voltage to the end lenses of the QLT. This provided axial containment to complement the radial containment provided by the main RF "quadrupole" trapping field, allowing simultaneous trapping of both anions and cations. To accommodate ion/ion reactions the instrument was reprogrammed to include the following sequence of scan events: cation injection, precursor ion isolation (within the linear quadrupole ion trap), anion injection, anion isolation, ion/ion reaction, and, finally, product ion mass analysis [12].

3. Results and discussion

3.1. Background

For the past decade ion/ion reactions have been extensively studied in the QIT, mainly by McLuckey and colleagues. Their work contains no reports of electron transfer from a singly-charged anion to a multiply-charged peptide cation. Instead, they describe proton transfer and anion attachment as the only observed reaction pathways following ion/ion reactions with peptide cations.

They did, however, make one report of electron transfer from singly-charged anions to multiply-charged precursors. The cation, doubly-protonated meso-tetra (4-pyridyl) porphine, was reacted with a mixture of anions derived from sulfur dioxide, namely $SO_2^{\bullet-}$ and $SO_3^{\bullet-}$ [16]. This produced both proton transfer, $[M+H]^+$, and electron transfer, $[M+2H]^{\bullet+}$ products; however, "very little if any fragmentation was observed". In a later review article, in reference to this result they state, "Note that there is essentially no evidence for fragmentation" [18]. In the same original paper they reported reaction of the triply-protonated neurotensin peptide, with either $SO_2^{\bullet-}$ or $SO_3^{\bullet-}$, resulted in only proton transfer [16]. Since we expected these anions to possess reasonably high gas-phase basicities, it was not surprising that proton transfer was the favored reaction pathway.

In that work, anions were generated with an atmospheric sampling glow discharge ion (ASGDI) source and admitted to the QIT through a hole in the ring electrode [16,18]. This radial injection scheme exposes the anions to kinetic excitation by the strong RF fields around the ring electrode. Anion injection, in their QIT device, was both "harsh" and inefficient since anions were subjected to fragmentation and loss through electron detachment. Therefore, the scope of available radical anions available to McLuckey and Stephenson was severely limited.

Based on our knowledge of negative ion chemical ionization [29,30] and a strategy for "gentle" anion production and injection [31] (NICI with QLT device), we believed the electron transfer reaction pathway was both viable and potentially useful. This belief was strengthened by a report of electron transfer from singly-charged anions to multiply-protonated peptides by Zubarev and co-workers [32]. In the early ECD experiments a gas, typically N_2 or Ar, was pulsed into the ICR cell to collisionally stabilize electrons during injection. In one experiment SF_6 was employed for electron thermalization. The entire reference is given below with the citations omitted:

*"**Anion Exchange.** Use of the heavier SF_6 in place of N_2 or Ar lowered the ECD product yield from ubiquitin +11 ions by a factor of ~ 8. A strong SF_6^- (m/z 146) peak was observed, again indicative of a high proportion of low-energy electrons: the maximum e-capture cross section of SF_6 is at 0.08 eV. Anion-cation reaction rates are several orders of magnitude slower than those for electron/cation; 30 s storage of SF_6^- with the +11 ubiquitin ion did produce near-normal e^- capture levels yielding reduced molecular ion, but with negligible (~ 1%) c,$z^\bullet$ production. This is further evidence for the importance of the excitation energy (~ 6 eV) supplied in electron capture (vide supra); for charge exchange by SF_6^-, the excitation would be lowered by the SF_6^- electron affinity value of 1.1 eV and also by the closer approach of SF_6^- before the e^- transfer."*

This passage reinforced our expectation that appropriately chosen radical anions – possibly $SF_6^{-\bullet}$ – could induce electron transfer and subsequently ECD-like fragmentation following reaction with multiply-protonated peptides. To pursue this assumption we constructed a novel ion/ion device centered around a QLT, placing emphasis on "soft" anion production and injection. And with it, we have recently demonstrated both the feasibility and utility of ion/ion chemistry for promoting a new type of ion fragmentation: ETD [12].

3.2. Anion specificity – background ions

Obviously, the sulfur hexafluoride radical anion was atop our list of promising candidates for electron transfer reagent anions. Thus, it was among the first anions to be reacted with multiply-protonated peptides on our QLT ion/ion device. In an early experiment, the triply-protonated phosphopeptide, LPISASHpSpSKTR, (m/z 482) was reacted (100 ms reaction time) with $SF_6^{-\bullet}$ radical anions to generate the doubly-protonated molecular ion, m/z 722, as the major product (Figure 1, avg. ~ 100 single-scan mass spectra). Evidence of electron transfer dissociation, however, can be found in the near-complete series of c/z-type product ions (confirmation of z_5 and c_7 is not possible since these are isobaric with the doubly-charged proton transfer product). Nonetheless, these products are present at low abundance. Note that while the bulk of the reagent anion population was comprised of radical anions of SF_6, low level background anions were also present (anion isolations were not performed at this point, data not shown).

This result was typical of our early work with other reagent anions including perflourotributylamine (FC-43) and perfluoro-1,3-dimethyl-cyclohexane (PDCH). Surprisingly, we always observed some ETD products no matter which reagent anions we used. During that time the ETD product yield was low and somewhat variable. Further, increasing the initial number of precursor cations did not enhance the absolute yield of ETD product ions. It did, however, result in a proportional increase in proton transfer product yield.

In a key experiment, we closed the SF_6 inlet and injected anions from background compounds in the NICI source. The resulting anion population comprised anions of residual SF_6, FC-43, PDCH, etc. among various unknown contaminants. That mixture provided more than a 10-fold increase in ETD product yield. Also ETD product yields became proportional to the initial precursor ion numbers. Obviously, in our early experiments, the contaminant anions, present at low relative abundances, accounted for production of the ETD products.

For unambiguous characterization of each reagent anion, we introduced a step of anion isolation prior to ion/ion reaction. Note, although segregated, both the anions and cations are simultaneously trapped during the anion isolation step. Thus, anions of m/z in the neighborhood of the cation precursor m/z are also retained. Despite this imperfection, the isolation step eliminates most of the unwanted reagent anions. With this approach, anions of a selected m/z (e.g., m/z 146 of $SF_6^{-\bullet}$) were reacted with selected multiply-protonated peptides (e.g., m/z 482 of LPISASHpSpSKTR).

Reaction of the isolated radical anion of sulfur hexafluoride with triply-protonated phosphopeptide, LPISASHpSpSKTR, generated only products of proton transfer (data not shown). Our result stands in contrast to those of Zubarev et al., described above. Dissimilar reaction conditions in the two devices are possible explanations for these differing results. For example, in our QLT instrument the $SF_6^{-\bullet}$ radical anions were collisionally cooled prior to ion/ion reaction. The lower pressure of the FTICR mass spectrometer presumably allowed the radical anions to persist in excited states during the ion/ion reaction. That residual excitation could render electron transfer more energetically favorable than proton transfer.

3.3. Sulfur dioxide

Introduction of sulfur dioxide to the NICI source generated the radical anion, m/z 64, along with m/z 83 – presumably $H_2SO_3^-$ (Fig. 2A). Radical anions of sulfur dioxide were isolated (Fig. 2B) and reacted with the triply-protonated neurotensin; the same peptide McLuckey and Stephenson reported for reactions with the same anion (vide supra) [16]. In our device, this reaction produced proton transfer products among numerous c/z-type fragment ions (Fig. 3, single-scan spectrum). Reaction of this anion with other peptides produced ETD-type fragments in all cases (data not shown). Reaction of m/z 83 with neurotensin cations does not yield detectable ETD product ions (data not shown).

3.4. Perfluoro-1,3-dimethyl-cyclohexane

The anion most frequently employed for ion/ion reactions by McLuckey and co-workers is perfluoro-1,3-dimethyl-cyclohexane (PDCH). Radial injection of that radical anion into the QIT generated a variety of PDCH-derived fragment ions, preserving little of the intact radical anion. With our QLT ion/ion apparatus the radical anion of PDCH is essentially the only m/z observed following injection and mass analysis (data not shown). Reaction of the PDCH radical anion with the triply-protonated phosphopeptide, LPISASHpSpSKTR, generates products corresponding to proton transfer only (Figure 4). Inspection of the isotope distribution of the singly-charged product near m/z 1443 reveals no evidence of charge-reduction via electron transfer.

Though our work employed the radical anion, it is doubtful the PDCH-derived fragment ions (employed by McLuckey et al.) would possess any greater proclivity for electron transfer. These results suggest the near exclusive use of PDCH for charge reduction of protein cations has likely prohibited any previous observations of electron transfer dissociation, assuming the process can occur in the QIT.

3.5. Anthracene

To date several potential anions have been tested for the ETD-inducing ability – anthracene has performed among the top. Figure 5 displays the anthracene anions generated and detected with our system, along with a structural interpretation. Injection, followed by a short 1 ms storage period in the QLT, produced the spectrum in Fig. 5A. Increased storage times, shown in Fig. 5B-C, display a conversion of m/z 177 to m/z 195, while m/z 179 remains unaffected. We believe m/z 177, the deprotonated anthracene anion, undergoes an ion-molecule reaction with water (in the QLT) to produce m/z 195. The radical anion of anthracene is not observed, but likely gets converted to m/z 179 through reactions with methane in the NICI source. Use of argon as the buffer gas neither produces the radical anion nor m/z 179.

Both m/z 177 and 179 induce ETD; both are even electron species. Reaction of m/z 179 with the multiply-protonated phosphopeptide, LPISASHpSpSKTR, produces extensive c/z-type fragmentation (Figure 6A), dissociation efficiency ~ 30 - 35% (precursor-to-ETD product). This anion induces similar dissociation efficiencies with all other multiply-protonated peptides where charge $\geq$ 3. Note proton transfer does occur following reaction of m/z 179 with phosphopeptide cations (see inset Fig. 6A); however, electron transfer without complete dissociation is also indicated by the enhanced abundance at m/z 1444.6 relative to m/z 1443.6. That m/z comprises both the undissociated single electron transfer product ($[M+2H]^{+\bullet}$) and the single ^{13}C isotope peak of the doubly-deprotonated peptide ($[M+H]^{+}$).

3.6. 9,10 diphenyl-anthracene

Proton transfer likely involves a closer approach between the anion and cation, relative to electron transfer, and requires the appropriate collision geometry. We expect less stringent requirements for electron transfer both in distance and geometry. To test this hypothesis, we employed 9,10 diphenyl-anthracene radical anions for the ion/ion reaction (anion spectrum Figure 7) with our standard phosphopeptide cation. Here the additional phenyl groups are oriented orthogonal to the central anthracene (not in the same plane). We expect the added phenyl groups would sterically hinder the site of negative charge for proton transfer reactions. Figure 6B displays the product ion spectrum resulting from reaction of the triply-charged phosphopeptide standard cations (m/z 482) with 9,10 diphenyl-anthracene radical anion (m/z 330). While the c/z-type fragmentation is comparable to that achieved with m/z 179 from anthracene, an increase in electron transfer without dissociation is observed (see inset Fig. 6B). Note electron transfer is increased at the expense of proton transfer.

Reaction of the quadruply-charged angiotensin (DRVYIHPFHL, m/z 325) with the radical anion of 9,10 diphenyl-anthracene (m/z 330) generates numerous c/z-type fragments among non-dissociated electron transfer products (Fig. 8). The first panel (Fig. 8A) represents the hypothetical isotopic distribution for the $[M+H]^{+}$ of angiotensin, placing it at m/z 1296.7. Figure 8B displays the singly-protonated molecular ion (full-scan MS), which has an isotopic distribution closely following the theoretical (Fig. 8A). The charge-transfer products resulting from ion/ion reactions with m/z 330 are skewed to higher m/z (Fig. 8C). This distribution results from ion/ion products of three consecutive charge transfer reactions and their associated isotopic distribution. They can be divided into four types of product ions: the products of three consecutive proton transfer reactions $[M+H]^{+}$ (~7%); two proton transfer and one electron transfer (any order) $[M+2H]^{+\bullet}$ (~17%); one proton transfer and two electron transfer (any order) $[M+3H]^{+\bullet\bullet}$ (~34%); and finally, three electron transfers $[M+4H]^{+\bullet\bullet\bullet}$ (~41%). The assigned percentages were obtained with a least squares fit of the isotopic peak clusters corresponding to each of these product categories to the spectrum in Figure 8C. The dominance of products corresponding to two and three electron transfer events, indicates that electron transfer is the primary ion/ion reaction pathway for 9,10 diphenyl-anthracene.

Isolation and collisional-activation (CAD) of cations corresponding to m/z 1299.6 generated a product spectrum comprised of both c/z and b/y-type fragment ions (data not shown). This data confirms that at least a portion of these charge-transfer product ions are non-covalently bound, yet dissociated precursor ions. Non-covalently bound charge-transfer products have been reported in the ECD literature [33-37].

At present, it remains unclear why the radical anion of 9,10 diphenyl-anthracene would provide increased electron transfer without (full) dissociation as compared to the anthracene m/z 179 anion. A heightened electron affinity of the molecule is one possibility, although, to our knowledge, these data are not presently known. Anion mass, a parameter that, as yet, remains untested, could also play a role in this process.

3.7. 3D vs. 2D traps for ETD

We originally surmised the process of electron transfer from anions to multiply-protonated peptides was anion dependent. We presumed anion choice, or lack thereof (due to the constraints of radial anion injection), had prevented others from inducing electron transfer in prior ion/ion work. With suitably-chosen anions we believed the process would be favored and would initiate dissociation analogous to ECD.

With this initial survey we have confirmed our guiding supposition: partitioning between proton and electron transfer is anion dependent. For example, the radical anion of PDCH promotes exclusive proton transfer while 9,10 diphenyl anthracene reacts with multiply-protonated peptides predominantly via electron transfer. In our QLT the radical anion of sulfur dioxide reacts with triply-protonated neurotensin to produce products of both proton and electron transfer. That same reaction in a QIT, described by McLuckey and Stephenson, reacted by proton transfer only. This disparity compels us to reassess our explanation of why ETD was not previously observed. At present we can offer only two explanations, neither of which is wholly satisfactory.

The QIT apparatus employed by McLuckey et al. had ~ 30-fold lower ion capacity than the QLT device used in our work. Spectral dynamic range, manifested by the ability to observe small peaks in an m/z spectrum, is directly proportional to trapped ion numbers. It is possible they lacked sufficient dynamic range to observe the low abundance ETD product ions. We assume their data were, to some extent, averaged; hence, if there were similar partitioning between proton and electron transfer for $SO_2^{-\bullet}$ we are not entirely convinced dynamic range would inhibit observation of electron transfer in their QIT.

A second possibility is a fundamental difference between the physics of ion motion in the two devices. This difference, alone or in combination with reduced dynamic range, could account for their null result. Ions trapped in a QIT are constrained by an RF pseudo-potential in all three dimensions. Ions in the QLT are constrained by an RF pseudo-potential in only 2 dimensions except when they venture near an end plate lens and come under the influence of its associated secondary pseudo-potential (during ion/ion reaction). For the most part ion motion along the QLT axis is constrained only by collisions with other ions and background gas molecules. Within trapping pseudo-potentials, the RF-induced micro-motion of nearby cations and anions is 180º out of phase. In the QLT, a portion of any given ion population will have motion primarily along the device's axis. The transverse RF micro-motion of those ions will be minimized – allowing positive and negative ions to have motion in the same direction. Thus, the statistical distribution of anion/cation relative velocities in the QLT is different from the QIT (more probability of having lower relative velocities). This difference may influence the dynamics of the cation-anion collisions and thus affect partitioning between proton and electron transfer.

4. Conclusions

Anion selection plays a critical role in effecting electron transfer dissociation (ETD) through ion/ion reactions with multiply-protonated peptides. In our ion/ion device, we find some anions react exclusively via proton transfer (e.g., $SF_6^{-\bullet}$), others react by both proton and electron transfer ($SO_2^{-\bullet}$, and m/zs 177, 179 from anthracene), while another behaved predominantly as an electron transfer agent (m/z 330; 9,10 diphenyl-anthracene).

9,10 diphenyl-anthracene shows improved electron transfer capacity, as compared to anthracene; however, the yield of dissociated, yet non-covalently bound product ions is increased. This result has two significant implications: (1) manipulations of anion structure can be effective in promoting selective ion/ion reactions (e.g., either proton or electron transfer) and (2) anion composition can affect the proportioning between complete dissociation and dissociated, but non-covalently bound (charge-reduced) products following an electron transfer event. The ideal ETD reagent anion would exclusively produce electron transfer with complete dissociation. With these results we expect, either by discovery or design, future research to identify anions that approach this ideal.

Anion selection, limited dynamic range, and differences in ion physics are possible reasons explaining why others have failed to observe electron transfer dissociation. Previous ion/ion work has relied upon radial anion injection into a QIT, a process which has limited the number of anions available for reaction. With our QLT apparatus the reaction of $SO_2^{-\bullet}$ with triply-protonated neurotensin generates c/z-type fragmentation. That same reaction, described by McLuckey and Stephenson in the QIT, produced only products of proton transfer. To establish whether the ETD process can be replicated on the QIT and to resolve these ambiguities further investigation with ETD-promoting anions, on the QIT, will be essential. In any case, their work including proton transfer, gas-phase concentration, and ion parking will likely play an important role, alongside ETD, in the application of mass spectrometry to proteomics.

Acknowledgment

The authors gratefully acknowledge the National Institutes of Health (DFH, GM37537 and AI33993;

JJC, RR018688), the National Science Foundation (DFH, MCB-0209793), and Thermo Electron for their generous support. We also thank Melanie Schroeder for assistance with the ESI setup, Scott Quarmby for donation of the batch inlet, and both Jim Stephenson and Neil Kelleher for helpful conversations.

References

[1] R. A. Zubarev, N. L. Kelleher, F. W. McLafferty, J. Am. Chem. Soc. 120 (1998) 3265-66.
[2] B. A. Cerda, D. M. Horn, K. Breuker, B. K. Carpenter, F. W. McLafferty, Eur. Mass. Spectrom. 5 (1999) 335-38.
[3] N. A. Kruger, R. A. Zubarev, D. M. Horn, F. W. McLafferty, Int. J. Mass Spectrom. 187 (1999) 787-93.
[4] E. Mirgorodskaya, P. Roepstorff, R. A. Zubarev, Anal. Chem. 71 (1999) 4431-36.
[5] N. L. Kelleher, R. A. Zubarev, K. Bush, B. Furie, B. C. Furie, F. W. McLafferty, C. T. Walsh, Anal. Chem. 71 (1999) 4250-53.
[6] A. Stensballe, O. N. Jensen, J. V. Olsen, K. F. Haselmann, R. A. Zubarev, Rapid Comm. Mass Spectrom. 14 (2000) 1793-800.
[7] S. D. H. Shi, M. E. Hemling, S. A. Carr, D. M. Horn, I. Lindh, F. W. McLafferty, Anal. Chem. 73 (2001) 19-22.
[8] E. Mirgorodskaya, H. Hassan, H. Clausen, P. Roepstorff, Anal. Chem. 73 (2001) 1263-69.
[9] B. A. Budnik, K. F. Haselmann, Y. N. Elkin, V. I. Gorbach, R. A. Zubarev, Anal. Chem. 75 (2003) 5994-6001.
[10] M. R. Emmett, J. Chromatog. A. 1013 (2003) 203-13.
[11] M. Mann, O. N. Jensen, Nat. Biotechnol. 21 (2003) 255-61.
[12] J. E. P. Syka, J. J. Coon, M. J. Schroeder, J. Shabanowitz, D. F. Hunt, P. Natl. Acad. Sci. USA submitted (2004).
[13] F. W. McLafferty, D. M. Horn, K. Breuker, Y. Ge, M. A. Lewis, B. Cerda, R. A. Zubarev, B. K. Carpenter, J. Am. Soc. Mass Spectrom. 12 (2001) 245-49.
[14] J. L. Stephenson, S. A. McLuckey, Anal Chem 68 (1996) 4026-32.
[15] J. L. Stephenson, S. A. McLuckey, Anal Chem 69 (1997) 3760-66.
[16] J. L. Stephenson, S. A. McLuckey, Int. J. Mass Spectrom. 162 (1997) 89-106.
[17] J. L. Stephenson, G. J. VanBerkel, S. A. McLuckey, J Am Soc Mass Spectr 8 (1997) 637-44.
[18] S. A. McLuckey, J. L. Stephenson, Mass Spectrom Rev 17 (1998) 369-407.
[19] J. L. Stephenson, S. A. McLuckey, Anal Chem 70 (1998) 3533-44.
[20] S. A. McLuckey, J. L. Stephenson, K. G. Asano, Anal Chem 70 (1998) 1198-202.
[21] R. Amunugama, J. M. Hogan, K. A. Newton, S. A. McLuckey, Anal Chem 76 (2004) 720-27.
[22] J. M. Hogan, S. A. McLuckey, J Mass Spectrom 38 (2003) 245-56.
[23] G. E. Reid, J. M. Wells, E. R. Badman, S. A. McLuckey, Int J Mass Spectrom 222 (2003) 243-58.
[24] M. He, G. E. Reid, H. Shang, G. U. Lee, S. A. McLuckey, Anal Chem 74 (2002) 4653-61.
[25] B. J. Engel, P. Pan, G. E. Reid, J. M. Wells, S. A. McLuckey, Int J Mass Spectrom 219 (2002) 171-87.
[26] G. E. Reid, H. Shang, J. M. Hogan, G. U. Lee, S. A. McLuckey, J Am Chem Soc 124 (2002) 7353-62.
[27] R. R. O. Loo, B. E. Winger, R. D. Smith, J Am Soc Mass Spectr 5 (1994) 1064-71.
[28] R. R. O. Loo, R. D. Smith, J Mass Spectrom 30 (1995) 339-47.
[29] D. F. Hunt, G. C. Stafford, F. A. Crow, J. W. Russell, Anal. Chem. 48 (1976) 2098.
[30] D. F. Hunt, F. A. Crow, Anal. Chem. 50 (1978) 1781-84.
[31] J. C. Schwartz, M. W. Senko, J. E. P. Syka, Journal of the American Society for Mass Spectrometry 13 (2002) 659-69.
[32] R. A. Zubarev, D. M. Horn, E. K. Fridriksson, N. L. Kelleher, N. A. Kruger, M. A. Lewis, B. K. Carpenter, F. W. McLafferty, Anal. Chem. 72 (2000) 563-73.
[33] D. M. Horn, Y. Ge, F. W. McLafferty, Anal. Chem. 72 (2000) 4778-84.
[34] K. Hakansson, H. J. Cooper, M. R. Emmett, C. E. Costello, A. G. Marshall, C. L. Nilsson, Anal. Chem. 73 (2001) 4530-36.
[35] M. Mormann, J. Peter-Katalinic, Rapid Comm. Mass Spectrom. 17 (2003) 2208-14.
[36] Y. O. Tsybin, M. Witt, G. Baykut, F. Kjeldsen, P. Hakansson, Rapid Comm. Mass Spectrom. 17 (2003) 1759-68.
[37] K. Hakansson, M. J. Chalmers, J. P. Quinn, M. A. McFarland, C. L. Hendrickson, A. G. Marshall, Anal. Chem. 75 (2003) 3256-62.

Figure Captions:

Figure 1. Product ion spectra following reaction of the triply-protonated phosphopeptide, LPISASHpSpSKTR, ($[M+3H]^{+3}$, m/z 482) with $SF_6^{-\bullet}$ (100 single-scan spectra, 100 ms reaction time). Note no anion isolation was employed during this reaction and other low-level background species were present.

Figure 2. Anions detected following introduction of sulfur dioxide into the NICI source (panel A, note SF_6 anions were residual from a previous exposure). Panel B displays mass spectrum generated following injection and isolation of the radical anion prior to ion/ion experiments.

Figure 3. Single-scan ETD product spectrum resulting from reaction of triply-protonated neurotensin (pELYENKPRRPYIL, pE represents pyroglutamic acid, m/z 559) with the radical anion of sulfur dioxide (m/z 64). Note numerous c/z-type fragments.

Figure 4. Reaction of m/z 482 (from LPISASHpSpSKTR, $[M+3H]^{+3}$) with the radical anion of PDCH. (A) Theoretical isotopic distribution of the singly-protonated peptide, and (B) inset of the charge-reduced ion/ion product. The radical anion of PDCH does not induce ETD at any detectable level (100 single-scan spectra).

Figure 5. Anions of anthracene generated following NICI with methane buffer gas. The first panel of the inset (A) represents the mass spectrum acquired following a short storage time (1 ms) in the QLT. Increasing the storage time to 500 ms reveals a reduction in m/z 177 with a comparable gain in m/z 195 (B). A one second storage replaces nearly all of m/z 177 with m/z 195. Also shown are structural

interpretations of the various detected mass-to-charges.

Figure 6. Reaction of m/z 482 (from LPISASHpSpSKTR, $[M+3H]^{+3}$) with isolated anions. (A) ETD product spectra (25 single-scan spectra) following reaction with m/z 179 of anthracene. (B) ETD product spectra (25 single-scan spectra) following use of the radical anion of 9,10 diphenyl anthracene, m/z 330. Note extensive c/z-type fragmentation in both spectra; however, m/z 330 induces increased electron transfer without dissociation (see insets).

Figure 7 Anions of 9,10 diphenyl-anthracene generated following NICI with methane buffer gas. Also shown is a structural interpretation of the detected anion.

Figure 8. Reaction of quadruply-protonated angiotensin (DRVYIHPFHL, m/z 325) with the radical anion of 9,10 diphenyl-anthracene. (A) Hypothetical isotopic distribution for the $[M+H]^{+}$, (B) Singly-protonated molecular ion of angiotensin (full-scan mass spectrum), and (C) charge-transfer product resulting from ion/ion reactions with m/z 330. Following ion/ion reaction, m/z 1299.6 (corresponding to three electron transfer events without dissociation) represents the most abundance m/z in that region (25 single-scan spectra).

Figure 1.

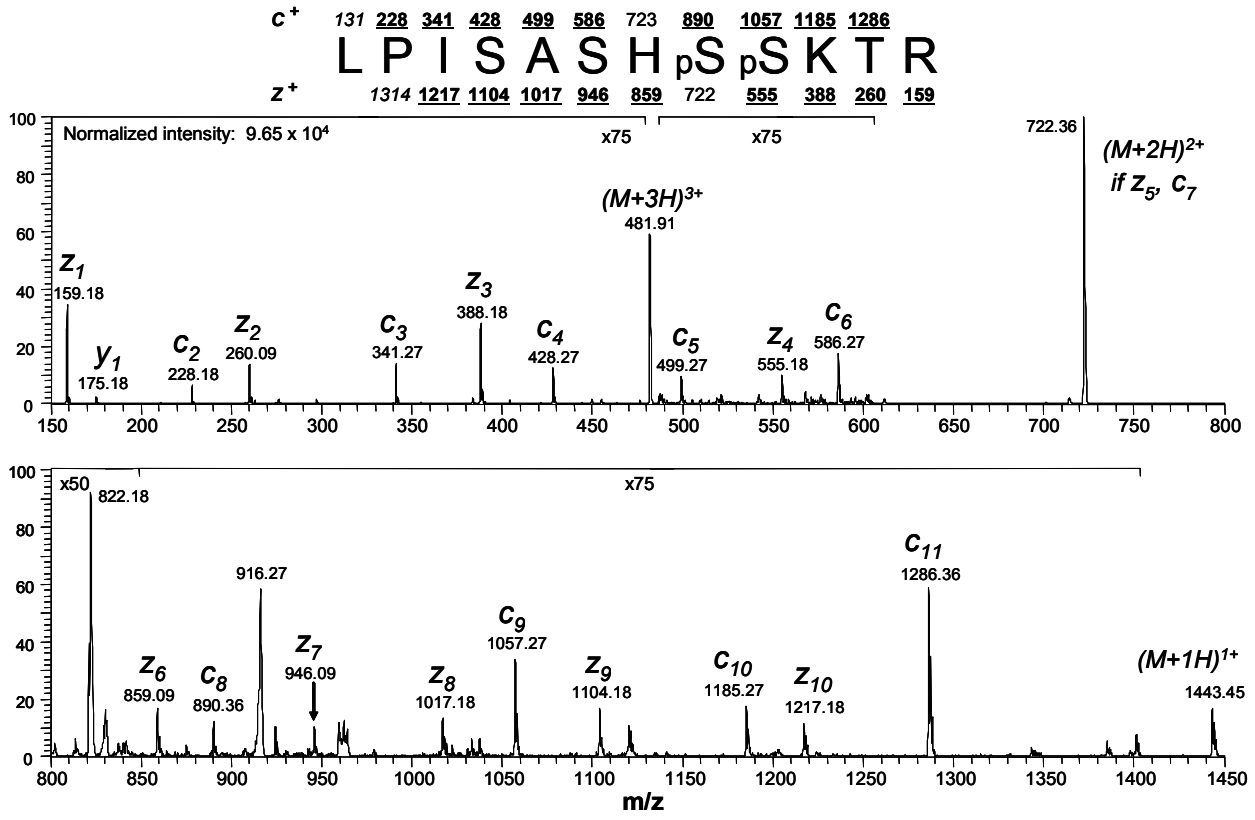
c+ 131 228 341 428 499 586 723 890 1057 1185 1286
L P I S A S H pS pS K T R
z+ 1314 1217 1104 1017 946 859 722 555 388 260 159
Normalized intensity: 9.65 x 10^4
x75
x75
722.36
(M+2H)2+
if z5, c7
(M+3H)3+
481.91
z1
159.18
y1
175.18
c2
228.18
z2
260.09
c3
341.27
z3
388.18
c4
428.27
c5
499.27
z4
555.18
c6
586.27
x50
822.18
x75
916.27
z6
859.09
c8
890.36
z7
946.09
z8
1017.18
c9
1057.27
z9
1104.18
c10
1185.27
z10
1217.18
c11
1286.36
(M+1H)1+
1443.45
m/z

Figure 2.

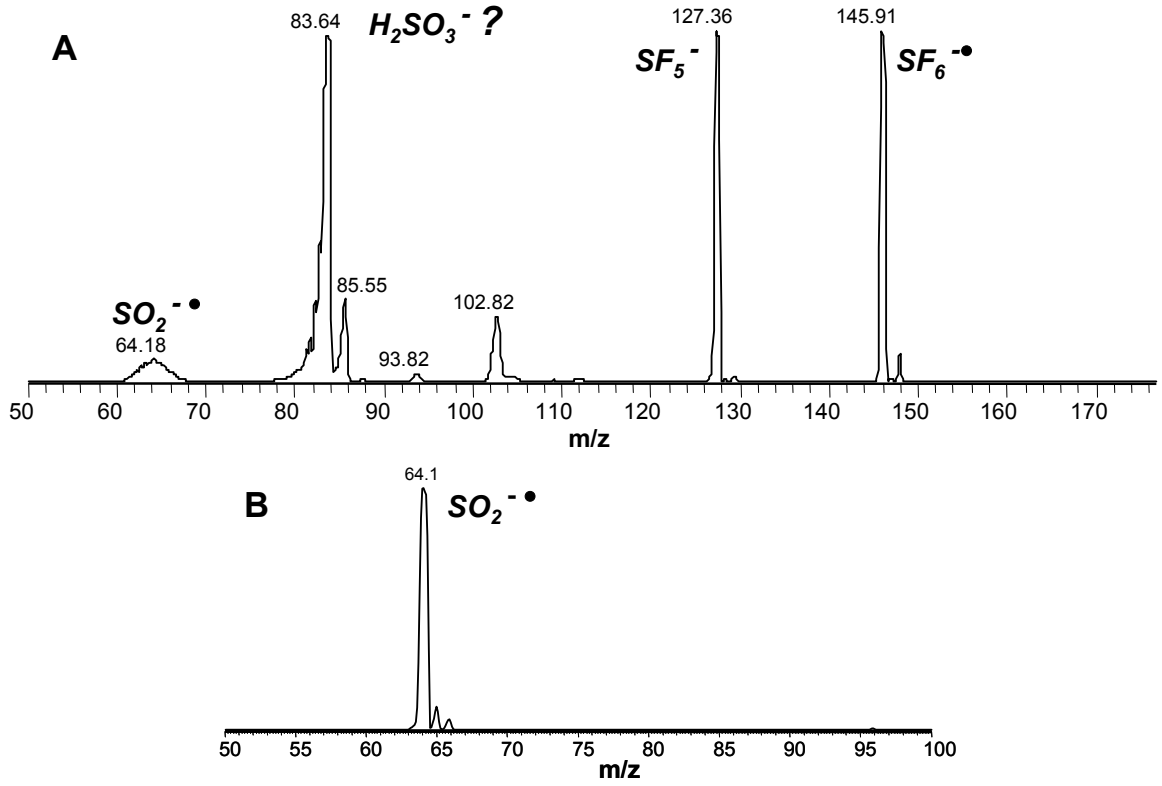
A
83.64
$H_2SO_3^-$?
127.36
SF_5^-
145.91
$SF_6^{-\bullet}$
$SO_2^{-\bullet}$
64.18
85.55
93.82
102.82
50 60 70 80 90 100 110 120 130 140 150 160 170
m/z
B
64.1
$SO_2^{-\bullet}$
50 55 60 65 70 75 80 85 90 95 100
m/z

Figure 3.

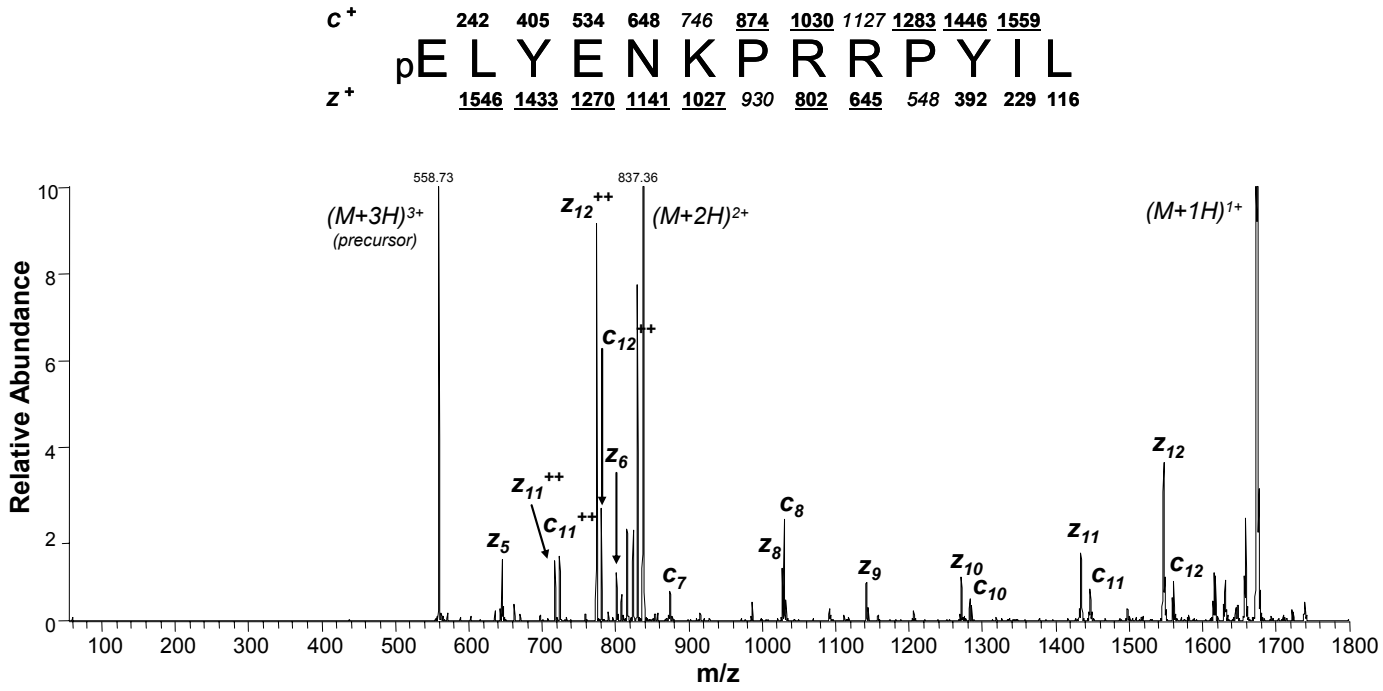
c+ 242 405 534 648 746 874 1030 1127 1283 1446 1559
pE L Y E N K P R R P Y I L
z+ 1546 1433 1270 1141 1027 930 802 645 548 392 229 116
Relative Abundance
m/z
(M+3H)3+
(precursor)
(M+2H)2+
(M+1H)1+
558.73
837.36
z12++
c12++
z6
z11++
c11++
z5
c7
z8
c8
z9
z10
c10
z11
c11
z12
c12

Figure 4.

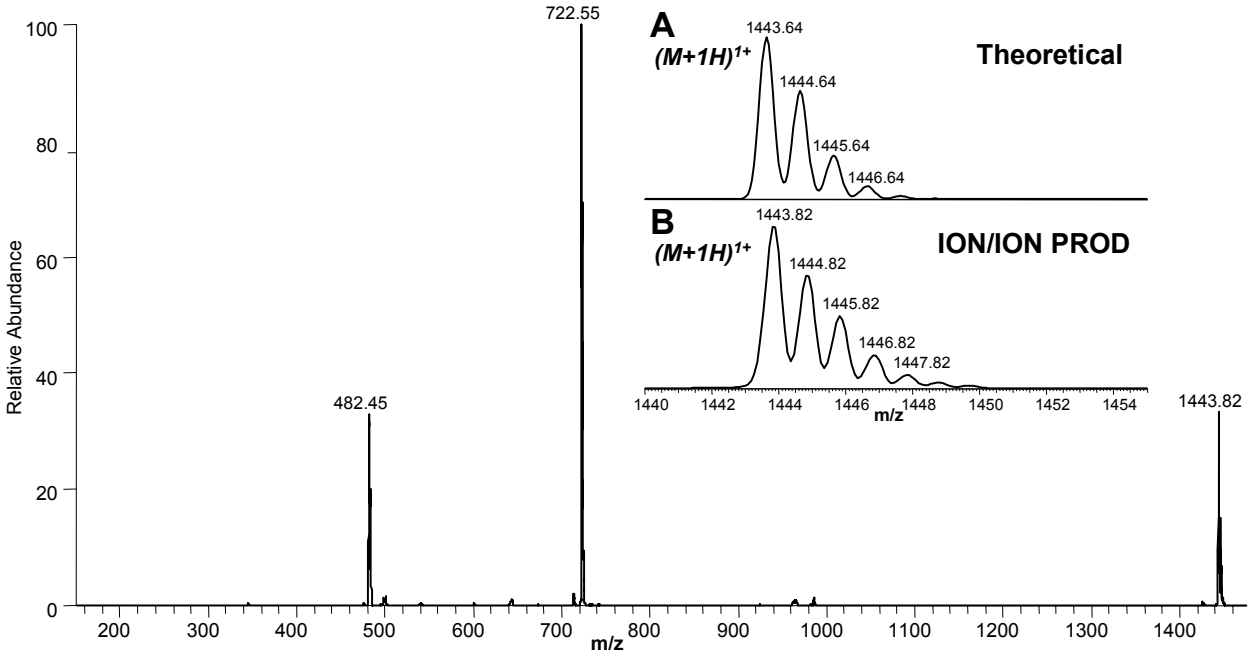
722.55
482.45
1443.82
Relative Abundance
m/z
A
(M+1H)1+
1443.64
1444.64
1445.64
1446.64
Theoretical
B
(M+1H)1+
1443.82
1444.82
1445.82
1446.82
1447.82
ION/ION PROD
m/z

Figure 5.

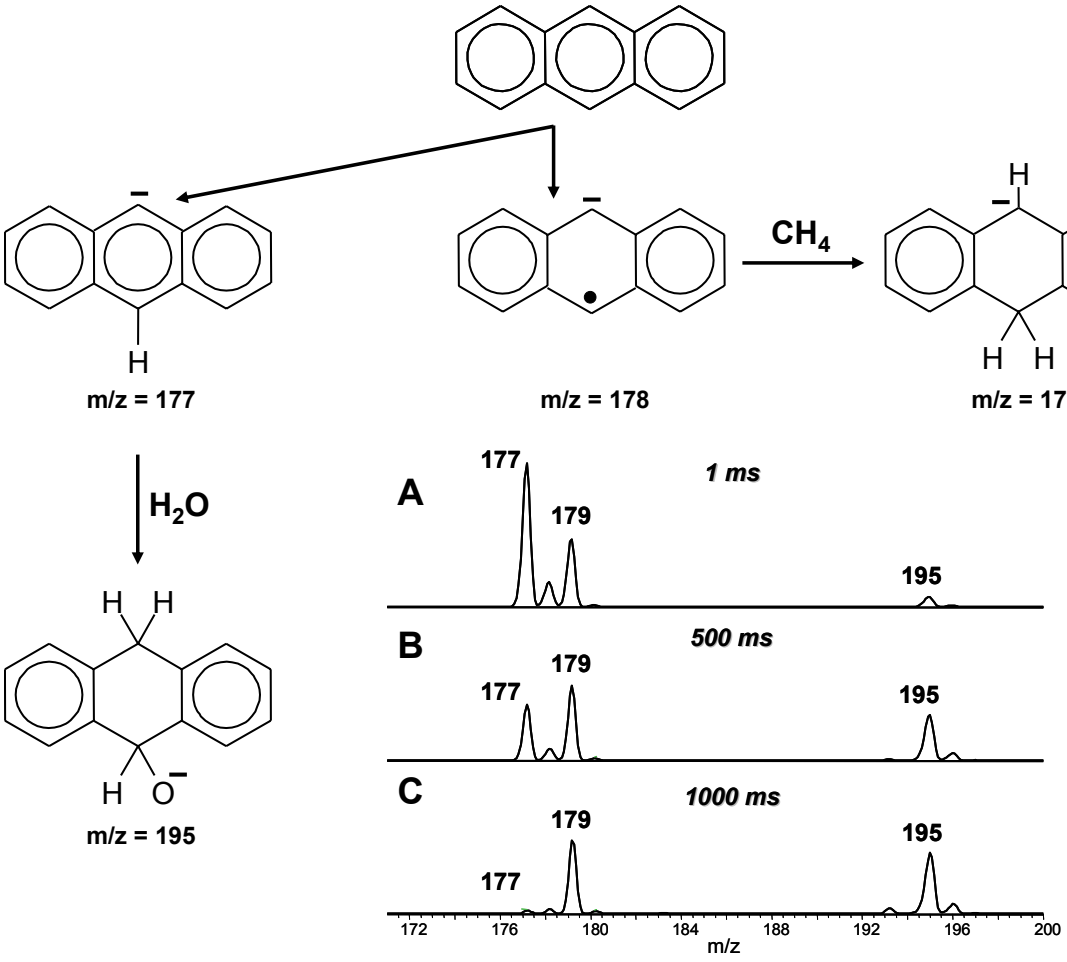
CH4
H
H H
m/z = 177
m/z = 178
m/z = 179
H2O
H H
H O
m/z = 195
A
1 ms
177
179
195
B
500 ms
177
179
195
C
1000 ms
177
179
195
172
176
180
184
188
192
196
200
m/z

Figure 6.

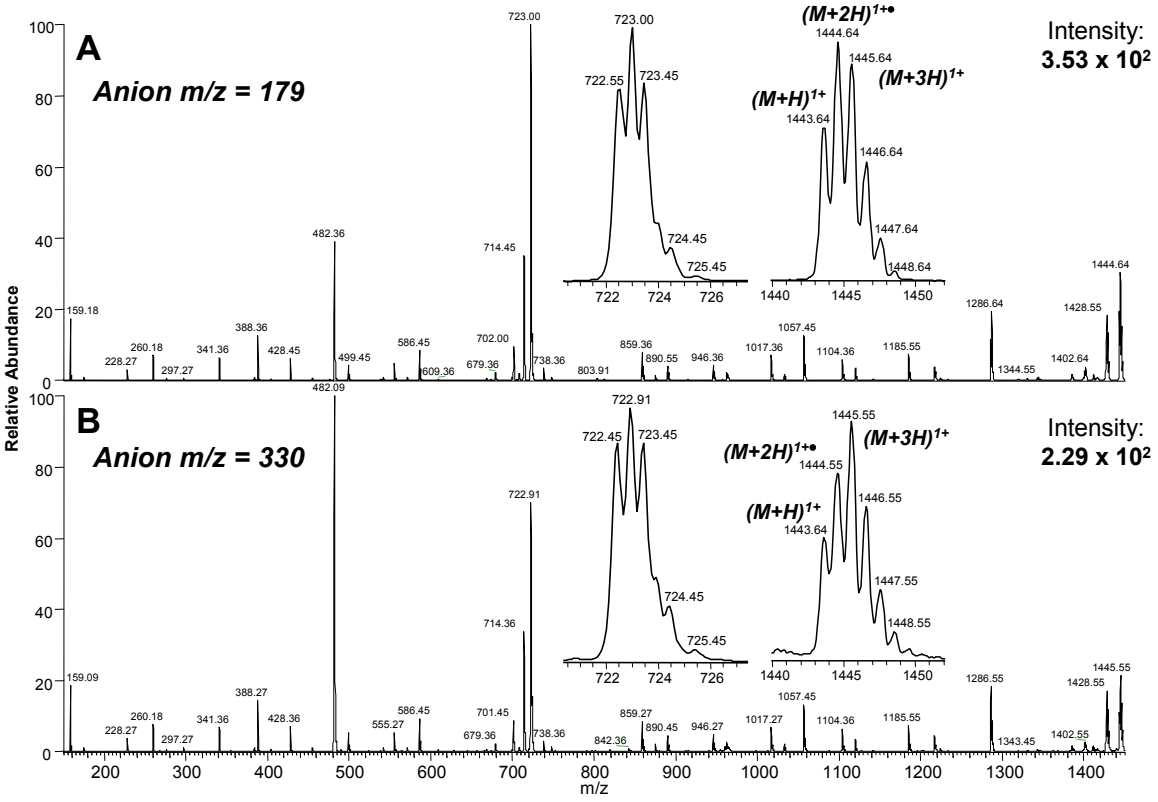
A
Anion m/z = 179
Intensity:
3.53 x 10²
(M+2H)¹⁺•
(M+H)¹⁺
(M+3H)¹⁺
B
Anion m/z = 330
Intensity:
2.29 x 10²
Relative Abundance
m/z

Figure 7.

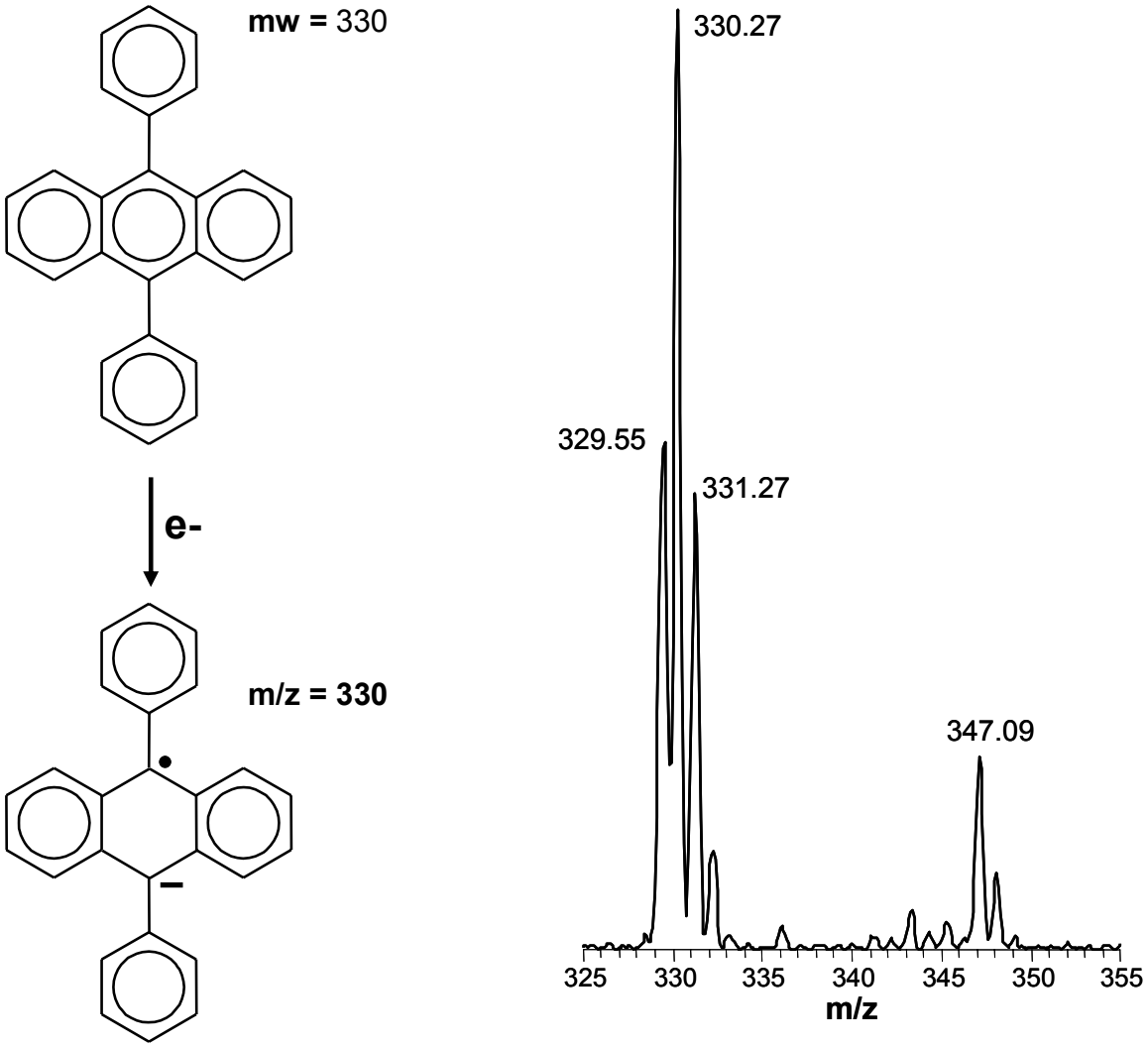
mw = 330
e-
m/z = 330
330.27
329.55
331.27
347.09
325
330
335
340
345
350
355
m/z

Figure 8.

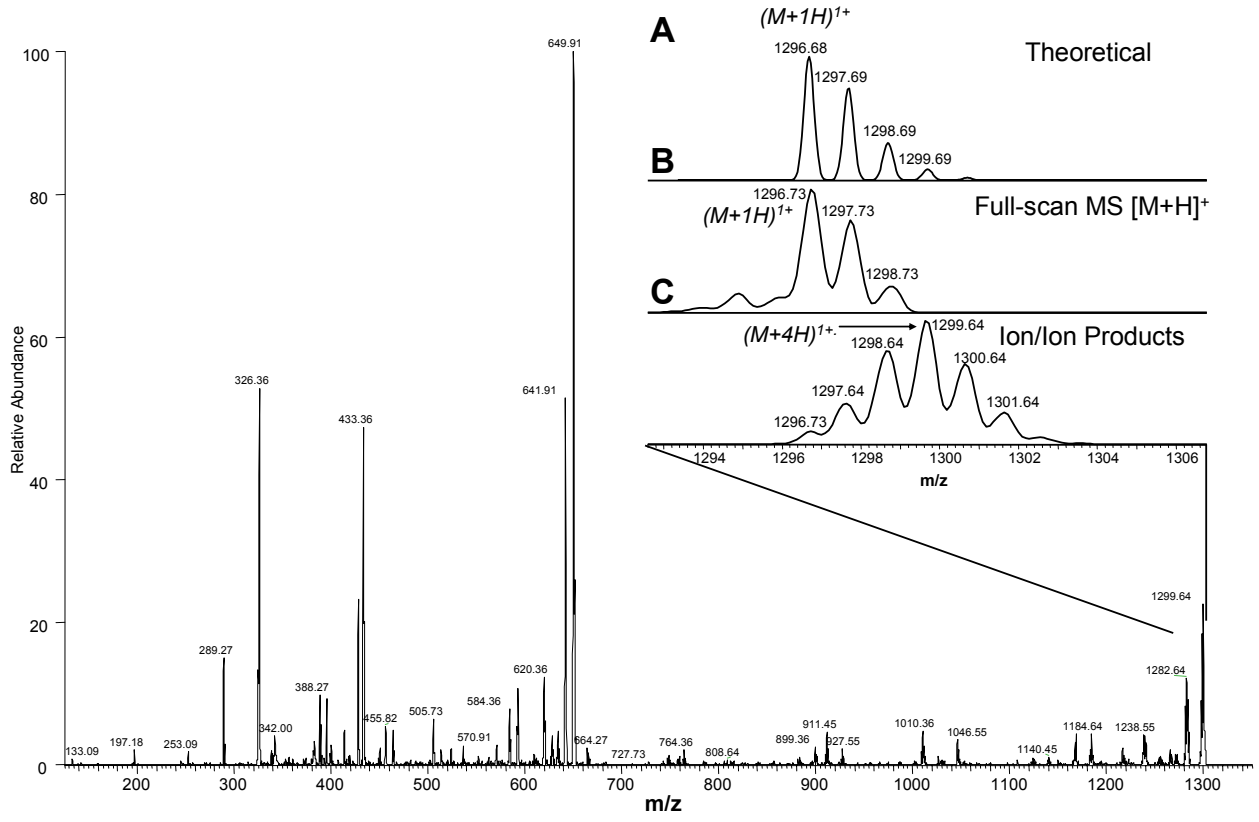
A
(M+1H)1+
1296.68
1297.69
1298.69
1299.69
Theoretical
B
1296.73
(M+1H)1+
1297.73
1298.73
Full-scan MS [M+H]+
C
(M+4H)1+.
1299.64
1298.64
1300.64
1297.64
1301.64
1296.73
Ion/Ion Products
1294
1296
1298
1300
1302
1304
1306
m/z
Relative Abundance
100
80
60
40
20
0
649.91
326.36
641.91
433.36
289.27
620.36
388.27
584.36
505.73
455.82
342.00
570.91
133.09
197.18
253.09
664.27
727.73
764.36
808.64
899.36
911.45
927.55
1010.36
1046.55
1140.45
1184.64
1238.55
1282.64
1299.64
200
300
400
500
600
700
800
900
1000
1100
1200
1300
m/z